FAILURE INVESTIGATION AND ANALYSIS OF LOCALLY MANUFACTURED TURBINE BLADE

Mahalaksmi Gunasilan¹, Shaiful Rizam Shamsudin^{1,*}, Rajaselan Wardan², Aleena Ramlee², Wan Mohd Haqqi Wan Ahmad² and Mohd Rafi Adzman³

¹Faculty of Mechanical Engineering and Technology, Universiti Malaysia Perlis (UniMAP), 02600 Arau, Perlis, Malaysia.

²Faculty of Chemical Engineering and Technology, Universiti Malaysia Perlis (UniMAP), 02500 Arau, Perlis, Malaysia.

³Faculty of Electrical Engineering and Technology, Universiti Malaysia Perlis (UniMAP), 02500 Arau, Perlis, Malaysia.

*rizam@unimap.edu.my

Abstract. This study aims to identify the root cause of a turbine blade failure after only 36 hours of operation and recommends measures to prevent future failures. The analysis involved four samples, including an OEM sample, three fabricated samples with cracks and parts, including a kept sample for failure analysis. Microstructural analysis using Villella's reagent as an etchant, surface morphology, and micro-elemental analysis were conducted using the benchtop SEM & EDS. The hardness of the samples was tested using the Rockwell (HRC) method. The failed blade was made of AISI 422 grade stainless steel. It failed due to chipping that initiated cracks when it was tightly fastened, facilitated by internal stress and intermetallic particles in the microstructure. Instead of turbine blades made of hardened steel, the material was found to be slightly ductile and highly prone to compression before breaking when over-tightened during assembly. Inadequate heat treatment practices caused varied microstructural patterns, including the presence of intermetallic particles and significant hardness differences between the fabricated and OEM samples, leading to internal stress. In order to prevent future failures, there is a requirement to improve quality control measures during the fabrication process, particularly in the aspect of heat treatment practices. Thorough testing and analysis of the material microstructure may also be necessary to identify and eliminate potential sources of internal stress and intermetallic particles. Proper installation and fastening of turbine blades, regular inspection, and maintenance can also help identify early signs of failure and prevent catastrophic failures from occurring.

Keywords: Failure, turbine blade, microstructural, hardness, chipping, cracks

Article Info

Received 3rd March 2023 Accepted 4th April 2023 Published 1st May 2023

Copyright Malaysian Journal of Microscopy (2023). All rights reserved.

ISSN: 1823-7010, eISSN: 2600-7444

Introduction

Turbine blades are radial aerofoils attached to the rim of a turbine disc, responsible for generating a tangential force that rotates a turbine rotor. These blades are present in gas turbine engines and steam turbines, which extract energy from high-pressure, high-temperature gas produced by the combustor. Due to the harsh environment, turbine blades use exotic materials like superalloys, as well as cooling systems such as internal and external cooling and thermal barrier coatings [1,2]. In power plants, gas turbine blades are exposed to extreme vibrations, pressure, and temperature.

The failure of turbine blade can significantly impact gas turbine engine safety, reliability, and efficiency. Manufacturers must conduct risk assessments to minimise losses due to failure. Rao et al. report that 42% of gas turbine engine failures are caused by blading issues [3], while Puspitasari et al. identify blade fatigue as the primary cause of failure in steam and gas turbines [4]. Fatigue arises from mechanical components experiencing stress due to vibration and resonance within the operational environment.

Turbine blade failure may result from high temperatures and pressures in the gas turbine combustion chamber due to direct flame exposure, limiting the blade's lifespan [5]. Carter et al. found that penetrating solid materials like detritus and other abrasive materials can prompt blade damage [6]. In thermal power plants, premature turbine blade failure is common. Yang et al. investigated martensitic stainless steel turbine blade cracking in a thermal power plant and found that inadequate heat treatment in the heat-affected and high-frequency hardening zones, resulting in uneven distribution of fine and coarse martensite, is the root cause of failure [7]. Similar failure conditions result from improper heat treatment in valve plugs used in power plants, causing sudden and premature service failure due to crack formation [8]. The microstructure of the interface's cracks exhibited significant carbide formation at the grain boundaries due to poor tempering heat treatment, resulting in the formation of acicular carbides at grain boundaries in the failed sample.

In the present case, the stainless-steel turbine blade was fabricated using the ladle technique to control the composition, distribution, and shape of intermetallic particles for improved machinability. The as-cast turbine blade was hardened at 1042 °C for one hour before being oil-cooled to below 66 °C. It was then tempered at 650 °C for 5.5 hours before being air-cooled again. The abnormal failure occurred when one of the operational turbine blades abruptly broke, leading to prompt termination of operation after 36 hours. Visual inspection revealed multiple fractured turbine blades.

The primary purposes of this article are to investigate the objective evidence presented by the failed components and to identify the root cause of the failure. Finally, strategies for corrective actions to avoid such shortcomings are addressed.

Materials and Methods

The chemical composition of the metal surface was analysed using an optical emission spectrometer, OES (Q8 Magellan, Bruker), after grinding the metal surface with 80-grit SiC paper. A digital DSLR camera (D3100, Nikon) was used for visual examination of the failed turbine blades (Figure 1). The investigated turbine blades' shape and dimensions

are shown in Figure 1(a) of the cracked sample, while Figure 1(b) displayed the appearance of the parted sample.

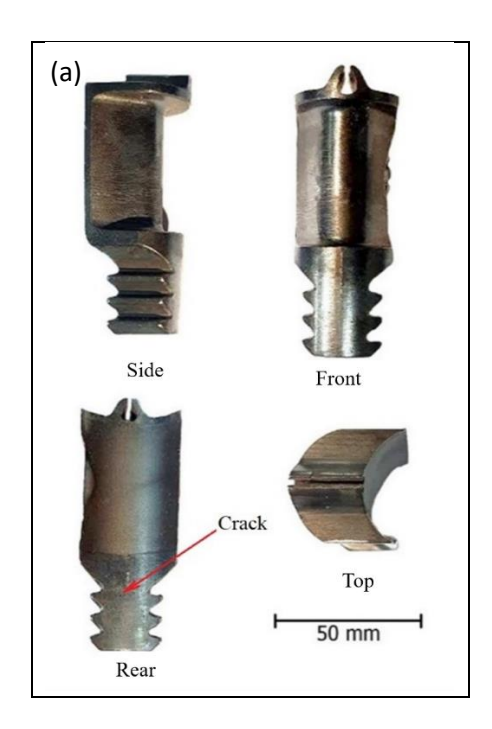




Figure 1: Camera photograph images of multiple viewpoints (top, side, front, and rear) for (a) cracked and (b) fractured turbine blade samples

To conduct a comprehensive examination of the failed sample, a stereomicroscope (SZX 10, Olympus) was used for close inspection. The analysis was performed on both the failed turbine blades fabricated by a local manufacturer (including a kept sample) and a brand-new turbine blade supplied by the original equipment manufacturer (OEM) sample. Both kept, and OEM samples were cross-sectioned, ground up to 1200 grit of SiC grinding paper, and then polished with a 6 and 1-micron diamond solution. A metallurgical microscope (BX41, Olympus) was used to assess the polished surface for any defects or microstructural abnormalities. Vilella's reagent (1 g picric acid, 5 ml hydrochloric acid, and 100 ml ethanol) was used to etch the samples, which were then examined again under a metallurgical microscope to identify specific microstructural characteristics. The surface morphology and micro-elemental analysis were conducted using the benchtop scanning electron microscope (TM 3000, Hitachi) & energy dispersive spectroscopy (EDS) (Xflash Min Sve, Bruker). Finally, the hardness test was performed using Rockwell HRC (206 RTD, Affri) at 15 different points for each sample, with calibration carried out using a standard block for hardness Rockwell C scale (N-6087, HRC 64.3).

Results and Discussion

Table 1 presents the chemical composition of the failed turbine blade steel, which conforms to the AISI 422 grade stainless steel. This martensitic, hardenable, high-alloy stainless steel exhibit excellent corrosion resistance and is typically used to manufacture components exposed to temperatures as high as 649 °C. Proper heat treatment can result in outstanding mechanical properties for components made from this steel, depending on their

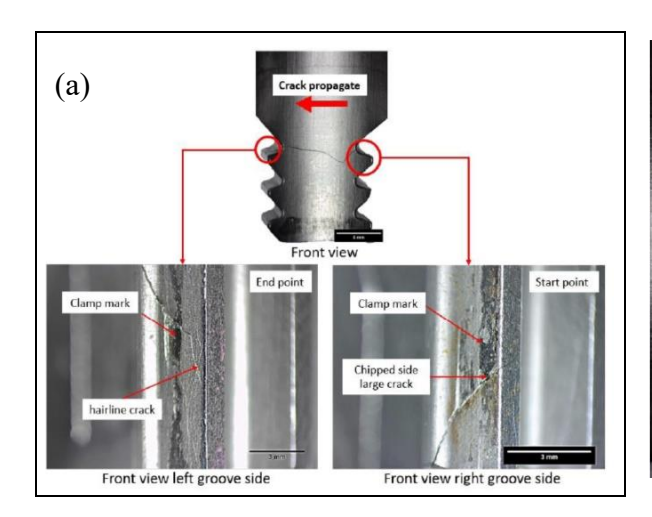
section, shape, and application [9]. AISI 422 stainless steel exhibits exceptional creep-rupture properties at temperatures up to 649 °C, in addition to its resistant against oxidation and scaling. When compared to other high-alloy steels of the martensitic type, AISI 422 stainless steel has the highest electrical conductivity and provides superior strength at elevated temperatures in contrast to AISI 403 steel.

| Element | Turbine Blade | |
|--------------|-------------------------|-----------------|
| | Failed turbine blade | AISI 422 |
| С | 0.21 | 0.20-0.25 |
| Si | 0.32 | 1.00 max |
| Mn | 0.74 | 1.00 max |
| Cr | 11.59 | 11.50-13.50 |
| Mo | 1.1 | 0.75-1.25 |
| Ni | 0.68 | 0.5-1.0 |
| \mathbf{W} | 0.96 | 0.75-1.25 |
| P | 0.02 | 0.040 max |
| S | 0.002 | 0.030 max |
| V | 0.23 | 0.20-0.50 |
| Fe | Bal. | ~ 82 |

Upon examination using a stereomicroscope, the threaded area surface of the turbine blade revealed a clamp-tightening effect, as depicted in Figure 2. The presence of chip marks on the right side of the blade's groove side indicates that the turbine has been tightened, putting the threaded area under pressure, as shown in Figure 2(a). The formation of cracks is visible in the threaded groove, where the stress is concentrated, with the crack initiating from the chipped area and propagating from the blade's right to the left side (Figure 2(b)). The nature of the crack propagation suggests that the failed turbine blade underwent compression. Further analysis showed that the turbine blade was not composed of fully hardened material, as evidenced by the crack pattern, which is indicative of ductile fracture. The presence of chip signs adds weight to the argument that the failure of this turbine blade is attributed to compression resulting from over-tightening. In addition to compression tightening, the operation that generates tangential forces to rotate the turbine, especially under high temperature and high-pressure gas conditions, facilitated crack propagation. Such tangential forces contribute to the formation and propagation of cracks, which ultimately leads to the failure of the turbine blade.

In Figure 3, a close-up stereomicroscope image of the parted turbine blade sample is presented. The image, shown in Figure 3(a), reveals that the fractured pattern of the parted sample is consistent with that of the cracked sample (as depicted in Figure 2(b)). Upon a cross-sectional view, the presence of shear lip features is evident, indicating that the material exhibits ductile fracture properties. This observation provides significant insight into the exact mechanism responsible for the failure pattern of the cracked and parted samples, both of which are fabricated samples. Further analysis of the surface fractography reveals that the fracture grain appears quite dull-rough grey (as depicted in Figure 3(b)). However, the deformation of the material surrounding the fracture is minimal, and the fracture surface seems smooth, with minimal shrinkage. These findings suggest that a significant transverse crack has developed, indicating that the failed turbine blade suffered a slight plastic residual

stress caused by compression due to over-tightening. Taken together, these observations suggest that the failure of the turbine blade was likely caused by a combination of factors, including over-tightening and the resulting plastic residual stress, as well as the material's inherent ductile fracture properties. These findings have important implications for the design and maintenance of similar turbine blades, as they underscore the importance of carefully controlling tightening forces and ensuring that materials are selected based on their specific properties and intended use.



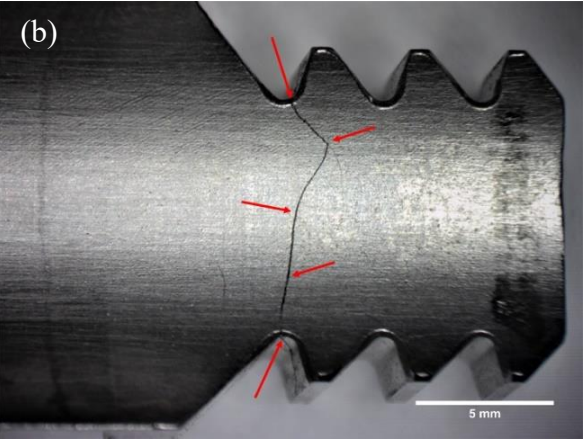
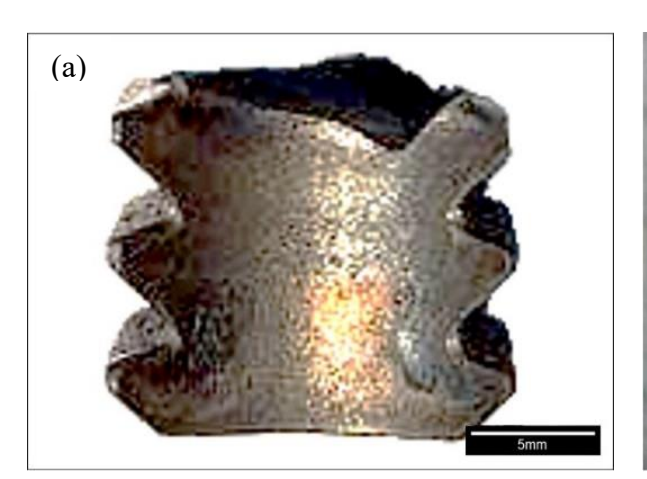


Figure 2: Stereomicroscope image of the cracked sample shows that (a) the crack propagation is visible across the threaded area and (b) crack across the body of the groove side of the turbine blade.



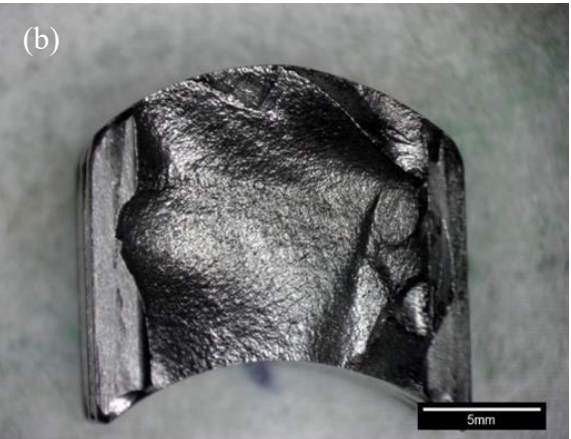


Figure 3: Stereomicroscope images on the parted sample: (a) side and (b) top view.

Figure 4 exhibits the microstructure images of the sample that was retained for further analysis. The as-polished kept samples, procured from local manufacturers, displayed intermetallic particles distributed throughout the metal matrix, as shown in Figure 4(a). In general, intermetallic particles can form during the manufacturing process and can negatively affect the mechanical properties of a material. The microstructure of the turbine blade has intermetallic particles that are believed to be composed of both carbides and silicides. However, the identification of these particles will be elaborated in the EDS findings. Upon etching the microstructure, it was observed that the intermetallic particles exhibited an

uneven, irregular, and coarser texture, with ferrite-free areas evident in the tempered martensite structure, as depicted in Figure 4(b). These intermetallic particles are unevenly distributed within the metal matrix. The presence of both carbides and silicides in the microstructure could significantly affect the material's properties and behaviour under stress, as these particles can act as crack initiators and propagate crack growth. This observation suggests that the presence of these intermetallic particles in the metal matrix may contribute to a decrease in the mechanical properties of the material.

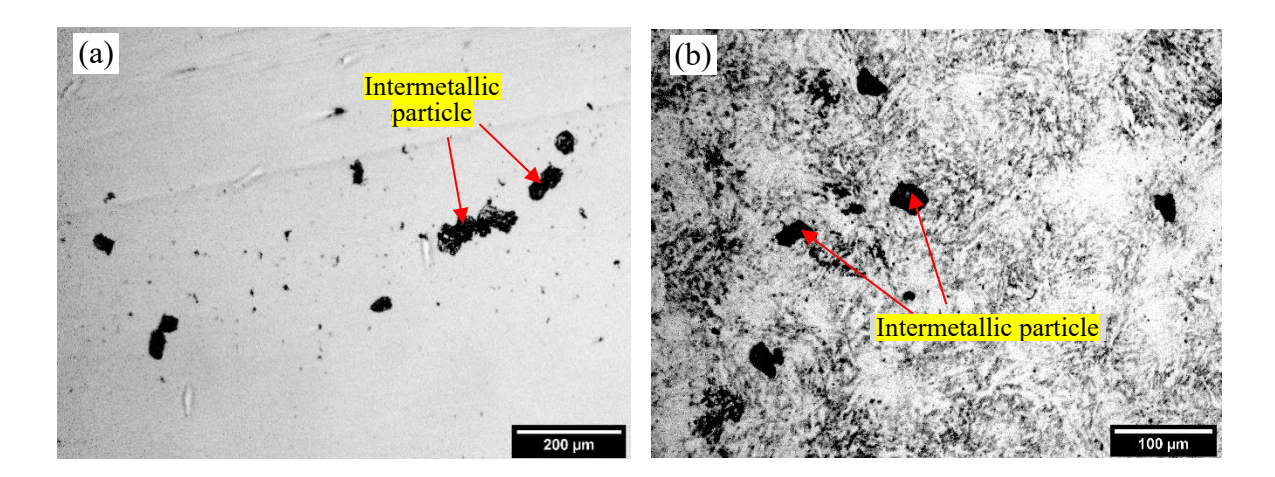


Figure 4: Optical metallographs of (a) as polished and (b) etched microstructure of the kept sample.

The microstructure of the OEM sample has a relatively smooth hardened stainless-steel structure, as shown in Figure 5. The as-polished microstructure of the OEM sample appeared to have a nearly perfect metal matrix, meaning that the metallic material appeared to have a homogeneous distribution of metal atoms throughout the entire material, without the presence of any voids or defects. Figure 5(a) shows that the microstructure of the OEM sample consisted mainly of a metallic matrix phase. The presence of a few subtle gray spots that appeared more contrasted than the matrix suggests the possible presence of a small amount of intermetallic, although it was not significant enough to affect the overall structure. It is likely that these intermetallic particles did not dissolve completely in the metallic phase during the heat treatment process. The absence of significant intermetallic particles in the OEM sample suggests that the material was manufactured with a high degree of purity and quality control, which is desirable for ensuring the consistent and reliable performance of the material.

The martensite structure of the OEM sample was found to be dense and dominated by fine carbides, with traces of delta ferrite evident, as depicted in Figure 5(b). The traces of delta ferrite would likely appear as distinct regions within the martensitic matrix, with a slightly different colour or texture compared to the surrounding material. The presence of these fine carbides in the microstructure contributed to the material's high hardness and brittleness, making it difficult for cracks to propagate. This observation is particularly significant as it implies that the OEM sample is capable of withstanding high stress conditions without undergoing material failure. Moreover, the presence of fine traces delta ferrite indicates that the sample was annealed after hardening, which effectively reduced residual stress in the material. The microstructure of the OEM sample, which is characterised by its high hardness and minimal intermetallic particles, makes it a promising material for various applications

that require excellent mechanical properties. The fine distribution of intermetallic particles and the presence of fine carbides in the martensite structure of the OEM sample make the material resistant to crack initiation and propagation.

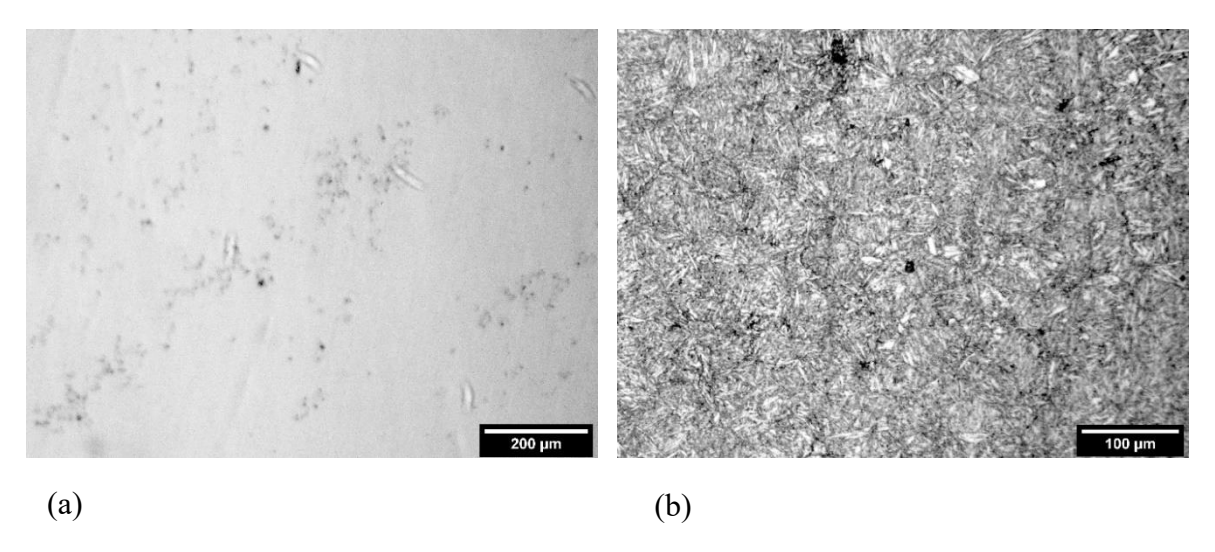


Figure 5: Optical metallographs on (a) as polished and (b) etched microstructure of OEM sample.

Figure 6 shows the intermetallic particles that are dispersed throughout the microstructure of the kept sample, as observed through close-up SEM analysis in Figure 6(a). Furthermore, Figure 6(b) presents the EDS pattern that display the elemental composition of the intermetallic particles, which comprises of carbon (C), silicon (Si), molybdenum (Mo), chromium (Cr), and iron (Fe). Based on the EDS results, it may suggest that the intermetallic black particles present in the martensite structure of the AISI 422 turbine blade are a combination of carbides and silicides. The 9.68 wt.% carbon detected in the EDS pattern indicates the possible formation of commonly found carbides in martensitic stainless steels, such as chromium carbides (Cr₃C₂) or iron-chromium carbides (FeCrC). In addition, the presence of silicon in the EDS pattern also suggests the formation of silicides, including chromium disilicide (CrSi₂) or ferrosilicon (FeSi). Nonetheless, the exact identity of these intermetallic particles remains inconclusive in this study. Thus, a more comprehensive analysis, such as X-ray diffraction or transmission electron microscopy, is necessary to determine their precise composition.

The OEM sample contains the same elemental components as the kept sample, with a comparable concentration. However, the significant difference between the two samples lies in the fine distribution of intermetallic particles in the OEM microstructure. Therefore, the observed variations in microstructural patterns between the OEM and kept samples are not due to differences in their chemical composition. Instead, manufacturing imperfections such as ladle casting procedures and heat treatment could have contributed to the formation of intermetallic solid particles in the stainless steel and different martensite structural patterns. It is believed that the imperfection of the heat treatment process plays a significant role in the production of intermetallics and the formation of martensite structures that have areas devoid of free-ferrite.

It is widely accepted that slow heating rates and proper preheating steps are beneficial for stainless steel. This is because most stainless steels are susceptible to thermal shock, and

rapid heating rates create thermal gradients that can cause them to crack. Additionally, stainless steels undergo a volume shift when heated to high temperatures, transitioning from their annealed microstructure to austenite. If this volume change occurs non-uniformly, it can cause unexpected distortion, especially when there are differences in section size. Therefore, for most stainless steels, it is recommended to choose a preheat temperature just below the material's critical transformation temperature and hold it long enough to ensure the entire cross-section reaches a uniform temperature. After preheating, the steel should be rapidly heated to the austenitising temperature. Babaei et al. demonstrated the efficacy of this method when they conducted preheat treatment on AISI 422 stainless steel at a rate of 8 K/min to 620 °C, held for 30 min, and continued heating with the same rate to the austenitising temperature of 1040 °C and 1070 °C, respectively [9]. Thus, the sudden failure of the operational turbine may have been caused by the lack of preheat treatment involving a slow heating rate to ensure uniform temperature throughout the cross-section, followed by an appropriate heating rate to reach the austenitising temperature.

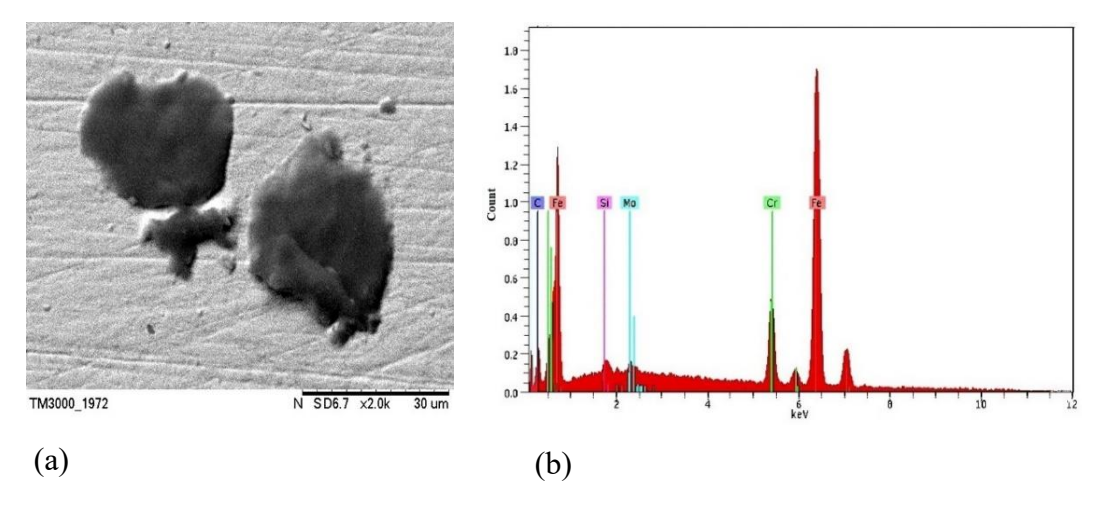


Figure 6: (a) SEM micrograph of intermetallic particles in the failed turbine blade and (b) EDS results of the elemental composition of the intermetallic particles.

The results presented in Figure 7 reveal some significant differences between the hardness values of the OEM turbine blade samples and the locally fabricated samples. The hardness readings for the OEM samples were found to be consistent across all the samples, indicating that they were subjected to a uniform heat treatment process, resulting in a consistent microstructure. On the other hand, the hardness readings for the locally fabricated samples, both the failed and kept samples, showed significant fluctuations. This variation in hardness can be attributed to the uneven microstructural patterns, indicating the presence of residual stresses resulting from conflicts in the heat treatment practices used during fabrication. Therefore, it can be concluded that the locally fabricated turbine blade is not comparable to the OEM sample due to the differences in their microstructure and hardness values. While the casting technique used in the fabrication process may not have been the source of the problem, it is clear that the heat treatment procedures employed in the local fabrication must be reviewed and optimised to ensure that they are comparable to the OEM turbine blade. Such a review and optimization of the heat treatment process will help ensure that the microstructure and hardness values of the locally fabricated turbine blades are consistent and comparable to those of the OEM sample, thereby improving the quality and reliability of the locally fabricated turbine blades.

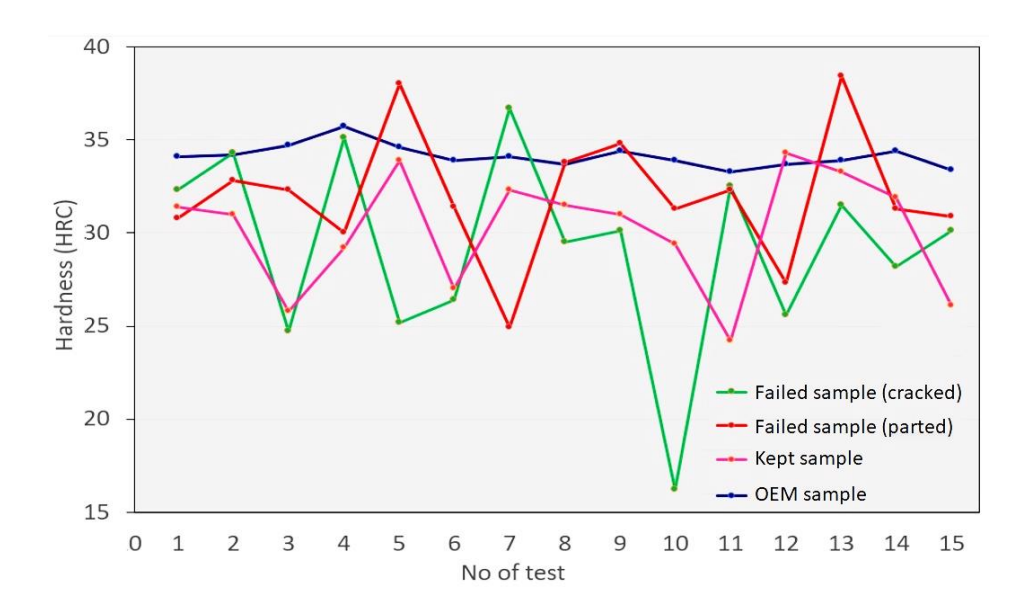


Figure 7: Rockwell hardness profile (HRC) turbine blade samples

As a recommendation, to obtain perfect, fully hardened stainless steel and reduce the risk of cracks or fractures, it is necessary to focus on several critical aspects, including the casting process, heat treatment, raw materials, and quality control. In this response, there are a few recommended preventive actions to be further insights on achieving the desired outcome. Firstly, to ensure the quality of the final product, it is crucial to remove all slag and dross during the casting process to prevent non-metallic inclusion contamination [10]. These contaminants can initiate cracks and lead to premature failure. Good casting practices, such as controlling the temperature and avoiding turbulence during the pouring process, should be implemented to prevent the formation of non-metallic inclusions. Additionally, to meet the operational requirements of the metal/alloy, the microstructure of the material should be designed accordingly. This can be achieved through advanced manufacturing techniques such as directional solidification and innovative heat treatment procedures, including quenching and tempering, to achieve the desired martensite microstructure and properties [11]. These measures can enhance the material's mechanical properties, minimise the risk of turbine blade failure, and increase the reliability and efficiency of the turbine operation.

Secondly, to improve the reliability and performance of turbine blades, it is recommended to ensure proper installation with the right amount of force or torque during the tightening process to prevent internal stress [12]. Thirdly, selecting high-quality raw materials is crucial to reduce the presence of intermetallic particles that can serve as crack initiators [13]. This includes using clean and pure raw materials free from sulfur, phosphorus, and nitrogen contaminants. Moreover, it is well known that the handling and processing of raw materials must be carefully monitored to ensure they are not contaminated during storage, transportation, or processing. This can be achieved by implementing proper handling and storage procedures and using dedicated equipment for handling raw materials.

Lastly, regular quality control and testing are essential to ensure the final product meets the specifications and standards. To achieve this, various tests, such as tensile, hardness, and impact testing, are conducted to verify the mechanical properties of the material [14]. In addition to these tests, microstructure analysis plays a crucial role in quality control. Manufacturers can compare a small sample of the product's microstructure with the

required microstructure and identify any deviations from the desired standard. Manufacturers can take corrective actions, such as adjusting processing and heat treatment procedures or selecting higher quality raw materials, to ensure the product's quality and reliability based on the deviations identified through microstructure analysis. Ultimately, microstructure analysis helps manufacturers minimise the risk of safety hazards or costly repairs while meeting the necessary specifications and standards.

Conclusions

In conclusion, imperfections in heat treatment practices during the fabrication process of turbine blades lead to the formation of intermetallic particles within the metal matrix. These particles act as crack initiators and facilitate crack propagation, ultimately leading to turbine blade failure. The microstructure and hardness variations of locally fabricated samples are attributed to internal stress induced by the imperfect heat treatment process. Failure occurs when the turbine blade is tightly fastened, creating chipping and cracks, facilitated by a combination of internal stress and intermetallic particles in the material microstructure. Therefore, it is crucial to ensure a consistent, precise, and perfect heat treatment process that satisfies the operational requirements of the turbine blade metal/alloy material and achieves the desired microstructure and properties. Quality control measures, such as random microstructure assessments and regular testing, can further ensure that the final product meets the required specifications and standards. Implementing these measures can minimise the risk of turbine blade failure, leading to a more reliable and efficient turbine operation.

Acknowledgements

The author would like to acknowledge the Fundamental Research Grant Scheme (FRGS) support under the grant number FRGS/1/2020/TK0/UNIMAP/02/85 from the Ministry of Higher Learning Malaysia.

Author Contributions

All authors contributed toward data analysis, drafting, and critically revising the paper and agreed to be accountable for all aspects of the work.

Disclosure of Conflict of Interest

The authors have no disclosures to declare

Compliance with Ethical Standards

The work is compliant with ethical standards

References

- [1] Rao, V. N. B., Kumar, I. N., & Prasad, K. B. (2014). Failure analysis of gas turbine blades in a gas turbine engine used for marine applications. *International Journal of Engineering, Science and Technology*. 6(1), 43-48.
- [2] Zhang, J., & Singer, R. F. (2002). Effect of hafnium on the castability of directionally solidified nickel-base superalloys. *International Journal of Materials Research*. 93(8), 806-811.
- [3] Rao, V. N., Kumar, I. N., Madhulata, N., & Abhijeet, A. (2014). Mechanical analysis of 1st stage marine gas turbine blade. *International Journal of Advanced Science and Technology*. 68, 57-64.
- [4] Puspitasari, P., Andoko, A. & Kurniawan, P. (2021). Failure analysis of a gas turbine blade. A review. *IOP Conference Series Materials Science and Engineering*. 1034(1), 012156.
- [5] Rao, N., Kumar, N., Prasad, B., Madhulata, N. & Gurajarapu, N. (2014). Failure mechanisms in turbine blades of a gas turbine Engine-An overview. *International Journal of Engineering Research and Development*. 10, 48-57.
- [6] Sellamuthu, R. & Giamei, A.F. (1986). Measurement of segregation and distribution coefficients in Mar-M200 and hafnium-modified Mar-M200 superalloys. *Metallurgical Transactions A*. 17(3), 419-428.
- [7] Yang, T., Xue, S., Zheng, L., Liu, L. & Liu, X. (2021). Crack investigation of martensitic stainless steel turbine blade in thermal power plant. *Engineering Failure Analysis*. 127, 105553.
- [8] Kalyankar, V. D. & Deshmukh, D. D. (2017). Failure investigations of failed valve plug SS410 steel due to cracking. *In IOP Conference Series: Materials Science and Engineering*. 282(1), 012007.
- [9] Babaei, H., Amini, K. & Shafyei, A. (2016). The effect of heat treatment on mechanical properties and microstructure of the AISI 422 martensitic stainless steel. *Mechanika*. 22, 576–580.
- [10] Wang, M., Song, B., Wei, Q., Zhang, Y. & Shi, Y. (2019). Effects of annealing on the microstructure and mechanical properties of selective laser melted AlSi₇ Mg alloy. *Materials Science and Engineering A.*739, 463–472.
- [11] Sames, W. J., List, F. A., Pannala, S., Dehoff, R. R. & Babu, S. S. (2016). The metallurgy and processing science of metal additive manufacturing. *International Material Reviews*. 61, 315–360.
- [12] Deters, C., Secco, E. L., Wuerdemann, H. A., Lam, H. K., Seneviratne, L. D. & Althoefer, K. (2013). Model-free fuzzy tightening control for bolt/nut joint connections of wind turbine hubs. In IEEE International Conference on Robotics and Automation, 270–276, May 2013.

- [13] Reddy, P. S., Kesavan, R. & Vijaya Ramnath, B. (2018). Investigation of Mechanical Properties of Aluminium 6061-Silicon Carbide, Boron Carbide Metal Matrix Composite. *Silicon*. 10, 495–502.
- [14] Lei, G., Wang, B., Lu, J., Wang, C., Li, Y. & Luo, F. (2022). Effects of solid solution temperature on the microstructure and properties of 6013 aluminum alloy. *Material Chemistry and Physics*. 280, 125829.